PERGAMON

Journal of Structural Geology 24 (2002) 1045–1053

JOURNAL OF STRUCTURAL GEOLOGY

www.elsevier.com/locate/jstrugeo

Finite-element modelling of shear zone development in viscoelastic materials and its implications for localisation of partial melting

Neil S. Mancktelow*

Department of Earth Sciences, ETH-Zentrum, CH-8092 Zürich, Switzerland

Received 20 November 2000; revised 2 April 2001; accepted 12 April 2001

Abstract

The development of shear zones initiating on random weaker initial perturbations is modelled numerically for low Deborah number viscoelastic materials, considering the influence of effective viscosity contrast, power law rheology, strain softening, and different imposed bulk deformation geometries, ranging from pure to simple shear. Conjugate shear zones initiate at ~90° to one another, and rotate with increasing bulk deformation, the basic pattern not being markedly influenced by the vorticity of imposed deformation. The rate of propagation of individual conjugate shear zones is little affected by increased effective viscosity contrast between matrix and inclusion but is promoted by power-law rheology. However, the most marked effect is observed for strain softening behaviour, where rapid propagation produces straighter and narrower shear zones. The localisation of strain is reflected in a correspondingly heterogeneous stress distribution. In particular, mean stress or pressure is higher in the extending, near planar, weaker zones of localised shear. Melting of gneissic or pelitic compositions is pressure dependent. With free water present, increased pressure promotes melting, whereas the opposite is true for water-absent melting. For water-present conditions, a positive feedback could develop between localised shearing, increased pressure and partial melting. This is potentially more effective in concentrating melt in shear zones than shear heating, where melt-related softening has a negative feedback effect.

Keywords: Shear zones; Finite-element modelling; Viscoelastic materials; Partial melting

1. Introduction

Shear zones, that is band-like structures of higher strain and vorticity than their surroundings, are common on all scales and may develop in apparently homogeneous and isotropic rocks (e.g. Ramsay and Graham, 1970; Cobbold, 1977; Casey, 1980; Poirier, 1980; Hobbs et al., 1990). Reflecting their importance to understanding rock deformation, there is a large body of existing literature considering the geometry and generation of shear zones (e.g. see the collection of papers in Carreras et al., 1980), but the mechanism of strain localisation in natural rocks is still not fully understood. One important question is the influence of initial perturbations and rock rheology on the pattern of shear zones that develop. Grujic and Mancktelow (1998) employed analogue scale models to investigate the geometry of shear zone localisation as a function of initial weak perturbation distribution. As for earlier results on individual shear zones (Baumann, 1986; Baumann and Mancktelow, 1987; Ildefonse and Mancktelow, 1993), networks of conjugate shear zones initially developed at 90° to each other, as expected for a pressure-insensitive viscoelastic rheology, and the angle between the shear zones progressively decreased with further deformation. However, in these analogue models the stress distribution could not be directly established. Gradual variation of material properties and boundary conditions was also impractical.

In high-grade terrains, partial melting and localised deformation of rocks are commonly interrelated. In field examples, melt (subsequently crystallised as leucosomes) may mimic original layering or it may be concentrated in shear zones, boudin necks or in the axial planes of minor folds (e.g. Brown et al., 1995; Brown and Solar, 1998; Kisters et al., 1998). The spatial distribution of these discordant structurally-controlled leucosomes cannot be due to initial variation in composition. Temperature variation, on the short length scales involved, is also an unlikely explanation for the observations. However, stress gradients associated with heterogeneous strain can be significant, even when the magnitudes of deviatoric stresses are small. Gradients in mean stress could produce a positive feedback between strain localisation in shear zones and

* Tel.: +41-1-632-3671; fax: +41-1-632-1030.
E-mail address: neil@erdw.ethz.ch (N.S. Mancktelow).

0191-8141/02/$ - see front matter
PII: S0191-8141(01)00090-6

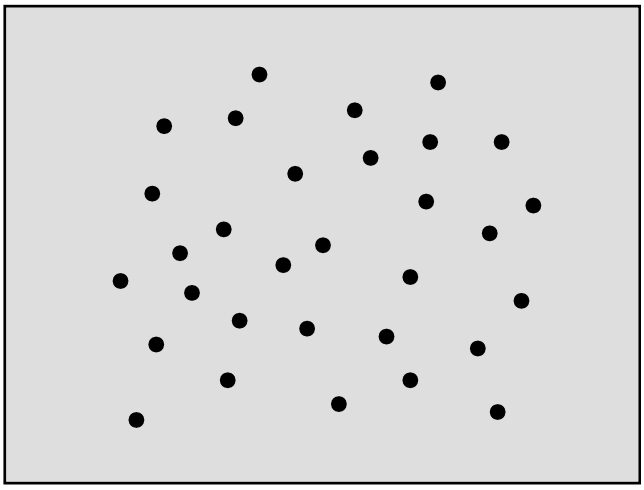

Fig. 1. Initial position of original weaker inclusions, chosen manually to represent an approximately random pattern. The initial shape is cylindrical, with a circular cross-section and cylinder axis parallel to the intermediate axis, which maintains a constant length in these plane strain experiments.

pressure-dependent phase transformations or metamorphic reactions lowering viscosity (Casey, 1980). Tectonically-induced pressure gradients have been previously proposed as a potential factor in melt generation and accumulation (e.g. Brown et al., 1995; Mancktelow, 1995), but the establishment of these gradients during deformation has not been rigorously modelled.

The current study extends the earlier analogue modelling work using finite-element numerical modelling to investigate parameters influencing shear zone initiation and geometry. The numerical models determine the spatial and temporal variation in stress during development of anastomosing shear zones for a range of viscoelastic material properties and boundary conditions between pure and simple shear. The results are relevant to shear zones in any viscoelastic material but are also considered here with special reference to melt generation and localisation in partially molten rock.

2. Model geometry and material rheology

All models are deformed in plane strain, in the range from pure to simple shear. For perfect pure shear, the two converging sides are maintained straight and parallel, whereas the two retreating sides are unconstrained. For all other experiments, the sides parallel to the shear direction are kept straight and parallel and the other two sides are linked, the y-coordinate being the same for corresponding nodes and the difference in x-coordinates being constant. This results in an effectively periodic model, repeating infinitely in the x-direction. The same distribution of initial perturbations is employed in all experiments (Fig. 1).

Rheological parameters are listed in Table 1. A Maxwell viscoelastic model is assumed, but Deborah numbers (e.g. see Poliakov et al., 1993) are low ($\leq$0.0125), approximating a nearly perfectly viscous material. The rheology is described by the equation

$$\dot{\bar{\varepsilon}}_{\text{creep}} = A\bar{\sigma}^{n}\bar{\varepsilon}^{m}_{\text{creep}}, \tag{1}$$

where the overbars refer to equivalent values, e.g.

$$\text{equivalent total creep strain} = \bar{\varepsilon}_{\text{creep}} = \sqrt{\tfrac{2}{3}\sum \Delta\varepsilon_{ij}\sum \Delta\varepsilon_{ij}}, \tag{2}$$

Δ indicating deviatoric values. Both linear and power-law viscous (stress exponent $n = 1$ or 3) behaviours are investigated, as well as the influence of strain softening (strain exponent $m = 0.8$) versus steady-state flow ($m = 0$).

3. Finite-element modelling

The commercial package MARC is designed for large strain non-linear problems (for details, see Mancktelow, 1999). In the current experiments, a four-node, isoparametric, arbitrary quadrilateral plane-strain element (element 11) is employed, except for the weak inclusions and their immediate vicinity, where the quadrilateral elements are decomposed into four three-node, isoparametric triangles (element 6). This finer mesh allows an accurate definition of the circular cross-section of the initial weaker perturbations, while maintaining a regular grid in the matrix. However, for some of the models approaching simple shear, this results in a 'checkerboard' pattern of mean stress values in the triangular elements (a common problem in finite-element modelling; e.g. Hughes, 1987). Since the

Table 1
Rheological parameters used in the numerical experiments. σ_{xx} is the normal stress parallel to the x-axis for pure shear deformation, De is the Deborah number $\mu\dot{\varepsilon}/G$, where μ is the effective viscosity, $\dot{\varepsilon}$ is the natural or logarithmic strain rate, and G is the elastic shear modulus. Poisson's ratio in all cases is 0.25. Note that the units chosen (MPa) are not critical for low De values as used here (i.e. effectively viscous behaviour). Scaling to Pa, for example, would produce identical results

Figure	σ_{xx} (matrix) [MPa]	σ_{xx} (inclusion) [MPa]	De (matrix)	De (inclusion)
2a	20	10	1.25×10^{-3}	6.25×10^{-4}
2b	20	0.2	1.25×10^{-3}	1.25×10^{-5}
3	200	0.2	1.25×10^{-2}	1.25×10^{-4}
5 and 6[a]	20	17.5	1.25×10^{-3}	1.09×10^{-3}

[a] Values at logarithmic strain $\varepsilon = -0.4$.

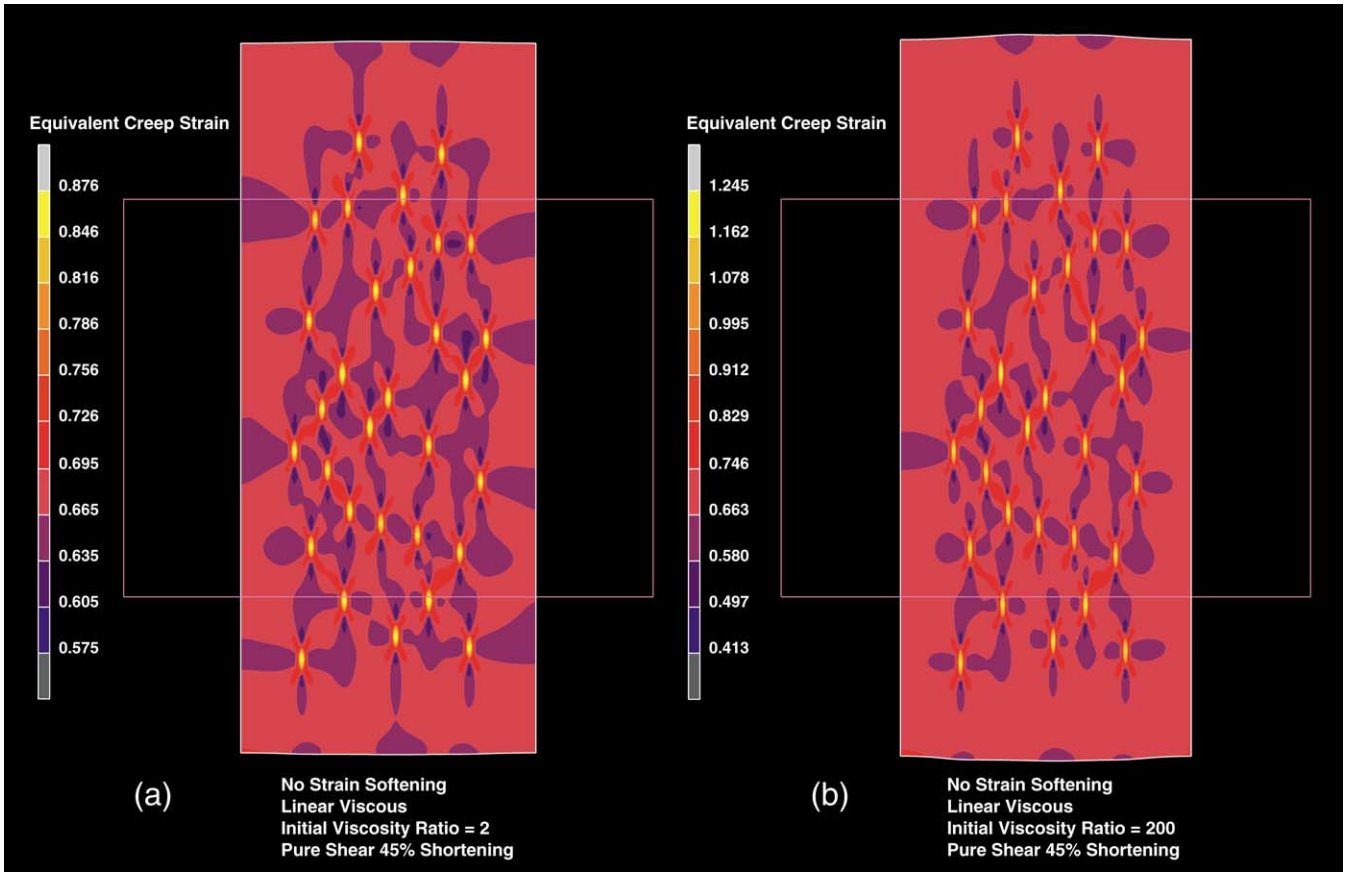

Fig. 2. Effect of viscosity contrast between inclusion and matrix (a: $R = 2$; b: $R = 200$) on the deformation pattern developed in pure shear for a linear viscous Maxwell material. Equivalent creep strain is defined by Eq. (2) in the text. Rheological parameters are listed in Table 1. Initial model shape given by faint rectangular outline.

interest is more in the mean stress distribution in the shear zones that have developed in the matrix between the inclusions, this is not an important issue. However, several control runs employed second-order elements (six-node triangle element 125 and eight-node quadrilateral element 27, respectively) to more accurately describe the mean stress distribution in the immediate vicinity of the inclusions. The results are not significantly different and vindicate the general use of computationally more efficient lower-order elements for the majority of runs.

4. Results

4.1. Effect of viscosity contrast

As can be seen from Fig. 2, the viscosity contrast between the weaker initial inclusion and the matrix has little influence on the strain pattern developed in the matrix. The only requirement for initiating heterogeneous deformation is the presence of an initial variation in material rheology. This need not be large. Indeed, in the experiments considered below involving strain softening, the initial perturbations were only ca. 20% weaker than the matrix and yet a heterogeneous shear zone pattern was rapidly established.

4.2. Linear versus power-law viscosity

Not unexpectedly (e.g. see Bowden, 1970; Poirier, 1980), power-law viscosity promotes localisation and the more distinct development of shear zones (Fig. 3). However, power-law rheology alone is insufficient to produce a clear pattern of anastomosing shear zones as observed in nature. The zones of higher strain and vorticity develop more-or-less symmetrically about the infinitesimal shortening direction, with an initial angle of 90° that increases with increased strain. This is as expected for a pressure-insensitive rheology and was also observed earlier in analogue scale model experiments using paraffin wax (Ildefonse and Mancktelow, 1993; Grujic and Mancktelow, 1998). Rotation of the shear zones with progressive deformation results in extension of the shear zones themselves, i.e. they become ‘stretching faults’ (Means, 1989). Such zones have a kinematic vorticity number W_k less than for simple shear (i.e. $W_k < 1$; Truesdell, 1953; Means et al., 1980). The lozenges of matrix between the shear zones must also deform as the shear zones rotate, progressively

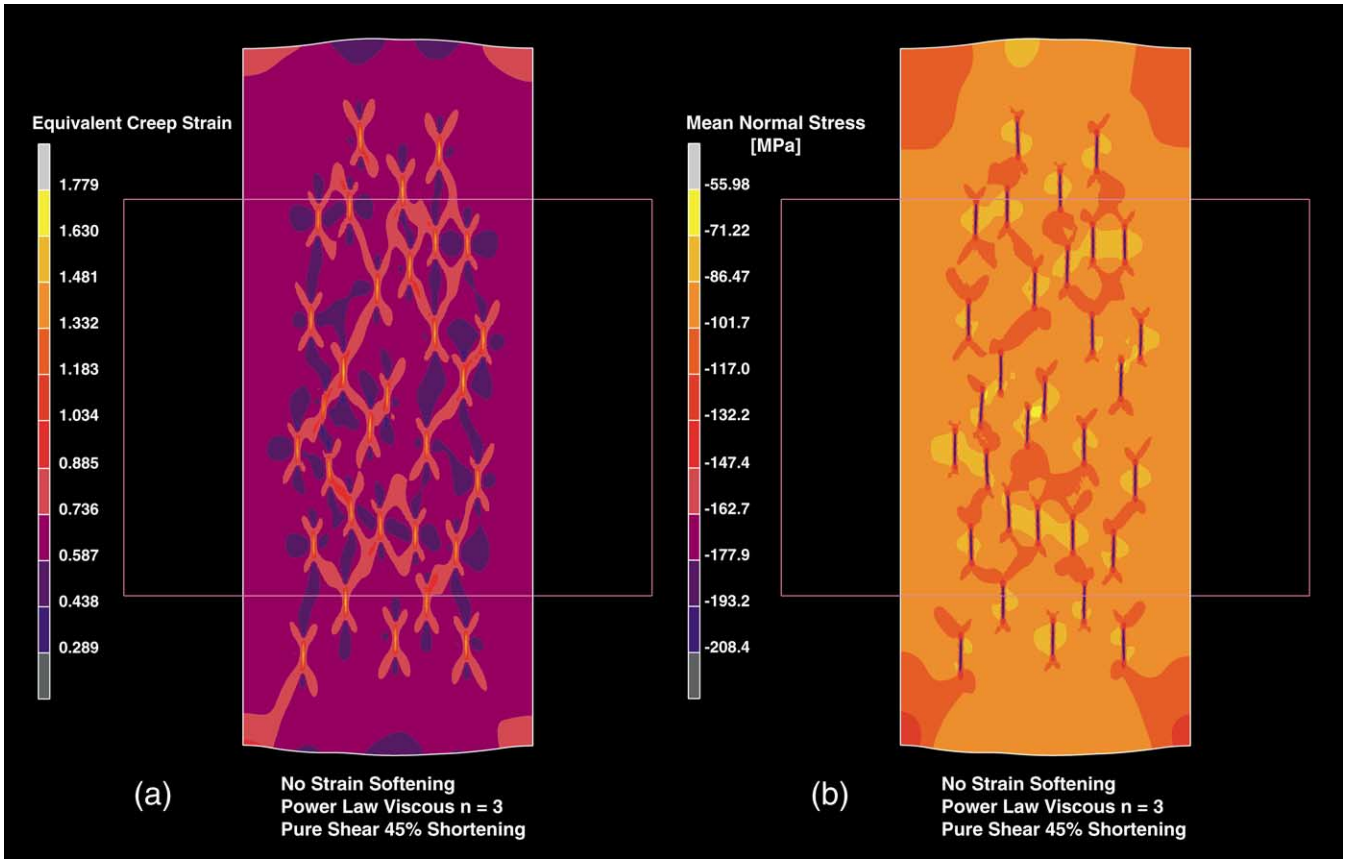

Fig. 3. Effect of power-law viscosity ($n = 3$ for matrix, $n = 1$ for inclusions) on the development of conjugate shear zones. Other rheological parameters in Table 1. (a) equivalent creep strain; (b) mean normal stress in MPa. Initial model shape given by faint rectangular outline.

changing from a rectangular to a more elongate diamond shape (Fig. 3a). Consequently, the difference in strain between shear zone and matrix never attains large values and actually tends to decrease with progressive deformation.

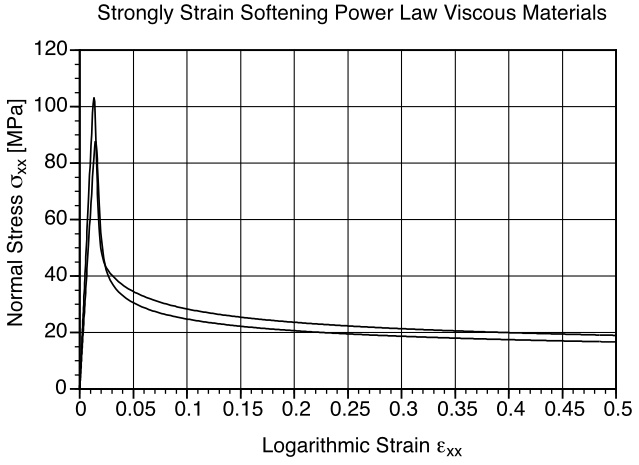

Fig. 4. Rheology of strain-softening materials employed in Figs. 5 and 6. In all cases, a power-law rheology with $n = 3$ for matrix and inclusions was employed. Strain softening corresponds to $m = 0.8$ in Eq. (1). Other rheological parameters in Table 1.

4.3. Effect of strain softening

Introducing strain-softening behaviour (Fig. 4) promotes the rapid establishment of a pattern of conjugate shear zones (Fig. 5), which are much straighter than in the steady-state case (cf. Fig. 3). Strong strain softening results in a growing rheological perturbation within the higher-strain shear zone itself, so that these zones can propagate without necessary regard for adjacent perturbations. In the current experiments, well-defined shear zones are only developed when there is marked strain softening during deformation. The geometry of the shear zone system is similar to that described in Section 4.2 above. The initial conjugate sets are at 90° and rotate with increasing deformation. Because material properties change with strain, the higher-strain shear zone itself effectively becomes another material and rotates as a material line. All such material lines rotate toward the finite extension direction and thereby into the field of infinitesimal extension, becoming stretching faults with $W_k < 1$.

4.4. Effect of boundary conditions (pure to simple shear)

In simple shear of an isotropic material, the initial positions of maximum shear stress (and infinitesimal shear

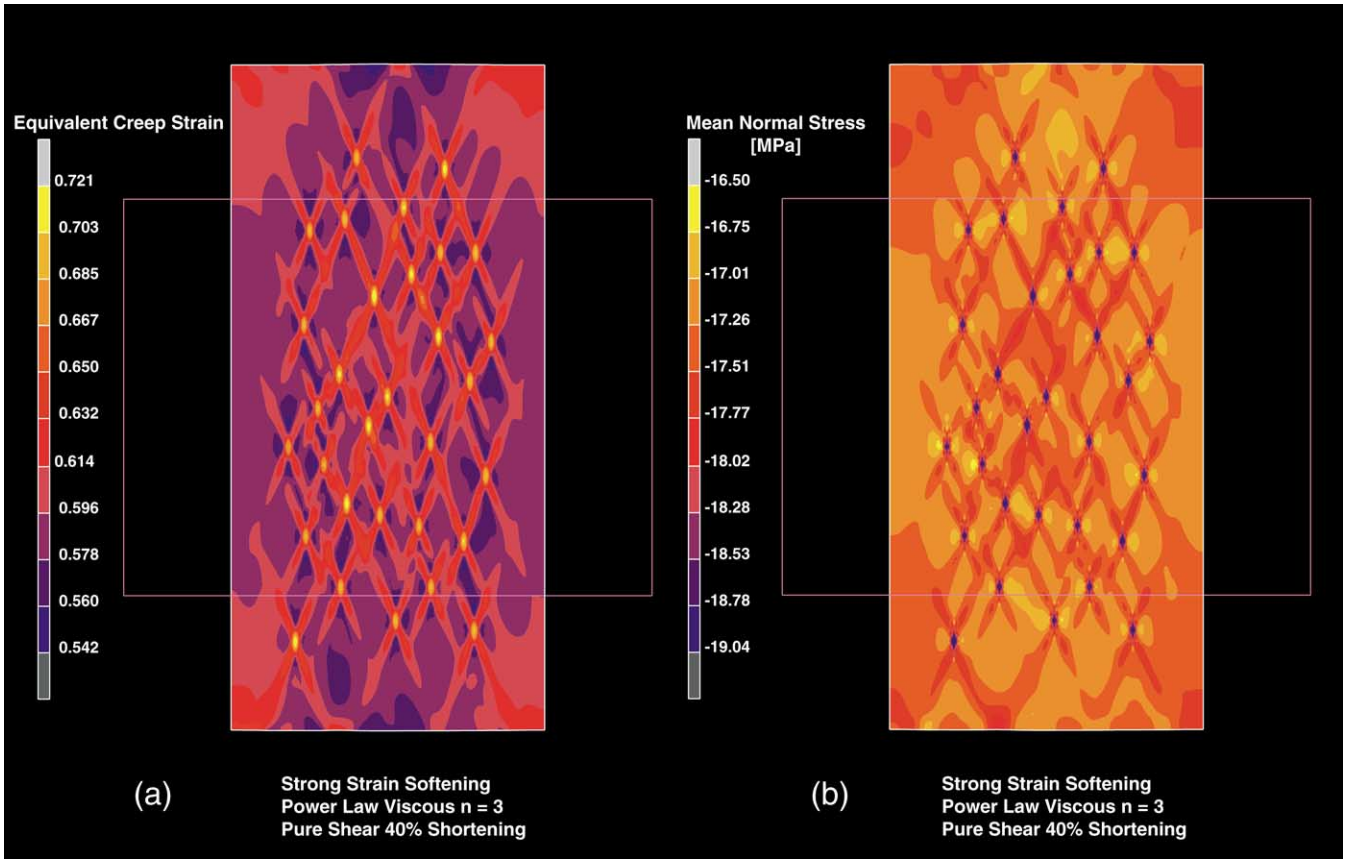

Fig. 5. Effect of strain softening (see Fig. 4) on the development of conjugate shear zones. (a) equivalent creep strain; (b) mean normal stress in MPa. Initial model shape given by faint rectangular outline.

strain) are parallel and perpendicular to the shear direction. The perpendicular orientation rapidly rotates (in fact it is the orientation with the highest rotation rate) and becomes a stretching fault as discussed above. The orientation parallel to the shear direction does not rotate, remains a plane of no longitudinal stretch and therefore can maintain a geometry near simple shear (Fig. 6a). The effect of even a minor amount of additional pure shear is to change the orientation of this zone, so that it now lies at a synthetic angle to the direction of imposed shear (Fig. 6b). The size of this synthetic angle increases slightly with increasing pure shear component (Fig. 6).

4.5. Mean stress distribution

For initial perfectly cylindrical perturbations, the mean stress in the weaker material is the same as in the unperturbed matrix and the stress distribution in the immediately surrounding matrix is the classic one for a weak inclusion or a hole, i.e. high mean stress on the sides facing the shortening direction and low mean stress facing the extension direction, with maximum shear stresses on the two perpendicular conjugate planes. As the inclusion deforms into an elliptical cross-section with long axis parallel to the finite extension direction, it approaches more and more the behaviour of a layer, with higher mean stress in the elongating weaker inclusion (e.g. Figs. 3b and 7; see Casey, 1980; Mancktelow, 1993). The shear zones in the matrix initiate parallel to the zones of maximum shear stress, for which the mean stress is equal to that in the undisturbed matrix. However, as noted above, a clear pattern of anastomosing shear zones only develops for strain-rate softening (i.e. power-law viscosity) or strain-softening behaviour. As these zones of localised deformation progressively rotate and are stretched, the mean stress in the weak shear zones becomes higher than in the adjacent matrix. For pure shear boundary conditions (Fig. 5), the shear zones and associated pattern in mean stress are symmetrical about the coaxial shortening direction. For a larger simple shear component (Fig. 6), the distribution is increasingly asymmetric, one of the conjugate pair of shear zones rotating into a direction of enhanced shear-zone-parallel stretch and the other rotating more slowly and remaining less stretched. For perfect simple shear, this second zone maintains an orientation nearly parallel to the bulk shear direction, i.e. a direction of no longitudinal stretch. As a result, for bulk deformation approaching simple shear, the mean stress is not clearly enhanced in the synthetic shear zone developed nearly parallel to the imposed shear direction (Fig. 6).

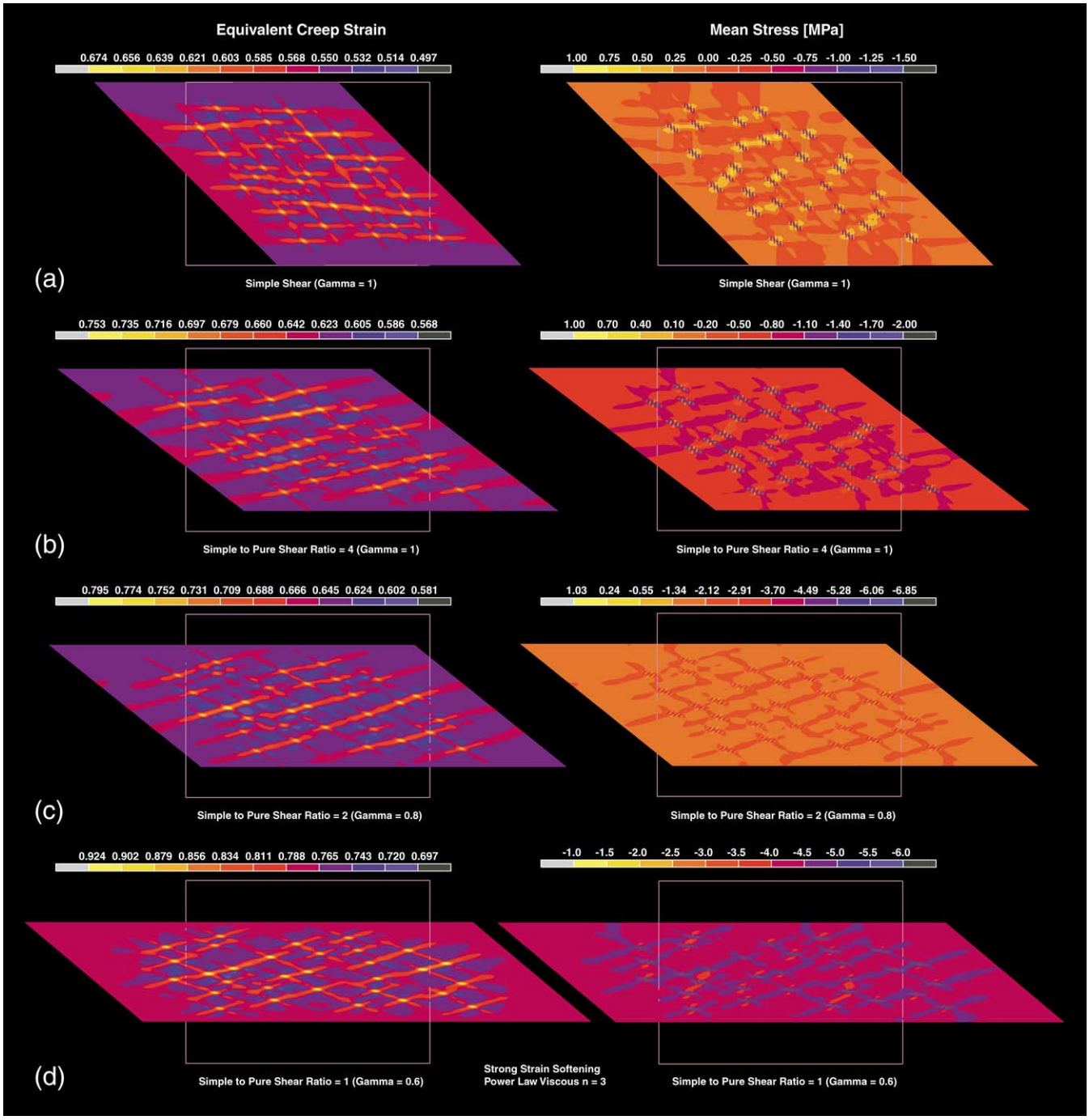

Fig. 6. Effect of imposed boundary conditions on the development of conjugate shear zones. Rheology as in Figs. 4 and 5. Initial model shape given by faint rectangular outline. Left and right columns show plots of equivalent creep strain and mean stress (MPa), respectively. (a) simple shear, $\gamma = 1$; (b) ratio simple to pure shear $= 4$, $\gamma = 1$; (c) ratio simple to pure shear $= 2$, $\gamma = 0.8$; (d) ratio simple to pure shear $= 1$, $\gamma = 0.6$.

For layers or elongate bands of differing rheology, the difference in mean stress between layer and matrix is approximately one half of the differential flow stress in the stronger material when the contrast in effective viscosity is high ($> \sim 10$, e.g. Fig. 7; Casey, 1980; Mancktelow, 1993). Mean stress is higher in the weak material when layers are extended (Fig. 7) and higher in the strong material when layers are shortened. Strain is generally localised in zones of lower effective viscosity (due either to strain or strain-rate softening). For stretching faults or thinning shear zones, as developed in the models considered here, the mean stress is therefore higher in the shear zone itself. For thickening shear zones, the pure shear component produces a stretch perpendicular to the walls. This could develop during asymmetric boudinage of layered or anisotropic materials or, on a larger scale, in detachment zones

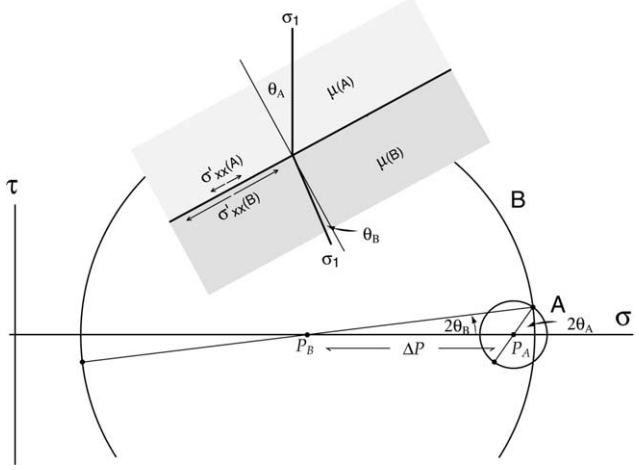

Fig. 7. Mohr representation of the stress state across a planar interface in extension. The shear stress parallel to the surface and the normal stress perpendicular to the interface must be the same for both materials, but the differential stress σ' and the normal stress parallel to the interface are different, reflecting the difference in rheology. The mean stress is therefore higher in the weaker layer, the difference ΔP approaching the value of $(\sigma_1-\sigma_2)/2$ in the strong layer as the contrast in material properties increases. Note also the concomitant refraction of the principal stress axis σ_1 in the stronger layer.

during synorogenic extension (e.g. Mancktelow and Pavlis, 1994). The Mohr circle stress representation for thickening shear zones is the mirror image of Fig. 7, the mean stress being lower in the shear zone than in the adjacent matrix.

5. Discussion

The geometry of the shear zones developed for pure shear boundary conditions is the same as observed in the directly comparable analogue model experiments of Grujic and Mancktelow (1998). However, in the current numerical experiments it was possible to vary material properties and boundary conditions to establish which parameters have a significant influence on the development of shear zones in viscoelastic materials. Of the parameters considered here, strain softening is the most important. This is in accord with the observations of Bowden (1970) and Hobbs et al. (1990) that, for pressure-insensitive (i.e. non-dilatant) rheology, localisation must occur in the strain softening regime. Weak dependence of the flow stress on strain rate (power-law viscous rheology or, in the limit, strain-rate independent plastic behaviour) aids localisation but is insufficient in itself (Bowden, 1970). However, although strong strain softening involving a five-fold reduction in flow stress with increased strain (Fig. 4) does produce a clearly defined conjugate shear zone pattern, the strain in the shear zones is only around 20% higher than in the matrix (e.g. Fig. 5a). This is not what is observed in natural examples, where there is often very strong strain localisation in shear zones (e.g. Ramsay and Graham, 1970). Increasing the simple shear component of the bulk deformation does not dramatically modify the results. In fact, there is little change in the pattern of conjugate shear zones as boundary conditions are varied between pure and simple shear, only a change in their orientation relative to the imposed boundaries (Fig. 6, left column). Unfortunately, this implies that the geometry of natural anastomosing sets of conjugate shear zones is probably not a useful criterion for establishing regional kinematics.

Shear zone development in partially molten rock is a special case of particular interest in high-grade metamorphic terrains. The numerical experiments presented here do not directly include the effects of phase transitions or consider rheology that varies with pressure. However, they do provide a basis for qualitative assessment of the potential for feedback between melting and strain localisation. Because melting curves are pressure dependent, gradients in mean stress (or 'pressure') that necessarily accompany heterogeneous deformation may determine the sites of syn-deformational melting. In this scenario, the variation in magnitude of mean stress is small but the gradients are still significant because of the short length scales involved. Pressure-induced localisation of melting in shear zones should produce a positive feedback effect: melting produces further weakening in the shear zone, aiding propagation and enhancing the further localisation of strain and the spatial variation in mean stress. This positive feedback may be far more effective in localising shearing and associated melting than proposed shear-heating models (e.g. Schubert and Yuen, 1978; Brun and Cobbold, 1980; Fleitout and Froidevaux, 1980), where the feedback is negative (because heating, melting and the resultant reduced effective viscosity reduces the further contribution of shear heating). Strain localises in weaker zones. If these zones are stretched (thinning shear zones or stretching faults), the pressure is higher in the shear zone; if they are shortened (thickening shear zones), the pressure is lower.

The examples modelled here are thinning shear zones. In this case, the higher pressure in the shear zones should tend to expel the melt developed, but as soon as melt moves down pressure and out of the region of greatest shearing it will solidify. This could further promote localisation, strain progressively concentrating along the still molten centre of the leucosome, while the walls have already solidified. In this scenario, melting is entirely dynamic — if deformation ceases, the melt immediately solidifies as the pressure variations rapidly decay. Such dynamic migmatites are not good sources for melt that could accumulate into major intrusive bodies. The melt remains trapped within the shear zones, since it would immediately solidify if it left the shear zones and attempted to migrate to higher crustal levels.

In general, water-present melting curves have a negative slope in pressure-temperature space and water-absent (i.e. incongruent melt reaction) curves a positive slope, at least at low to moderate pressures (Fig. 8; Tuttle and Bowen, 1958; Brown and Fyfe, 1970; Holtz and Johannes, 1994; and many

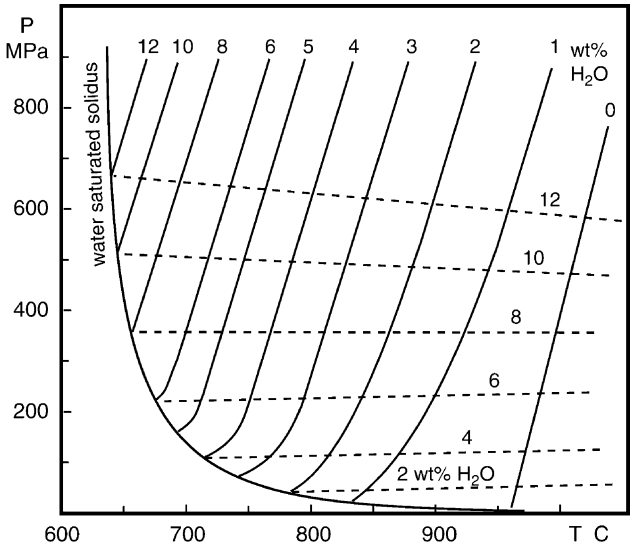

Fig. 8. Water-saturated solidus curve, liquidus curves for a given amount of H_2O, and H_2O solubility curves (dashed lines) in the system quartz–albite–orthoclase–H_2O for minimum and eutectic compositions, redrawn after Fig. 2 from Holtz and Johannes (1994).

others). The solubility of water in granitoid melts increases with increasing pressure (e.g. Holtz and Johannes, 1994). It follows that, although increasing pressure aids initial transgression of the water-present melting curve, further increase in pressure above the solidus results in a reduction in the amount of melt present. However, the reduction is only small for the small magnitudes of mean stress variation appropriate to partial melts (Fig. 9), and the most important effect should remain the localisation of initial melt development as the solidus is crossed in areas of slightly enhanced pressure.

Casey (1980) predicted that syn-deformational transformation to phases stable at higher mean stress could cause ductile shear zones to develop at angles >45° to the regional σ_1 direction and transformation to phases stable at lower mean stress could result in angles <45°. For water-absent melting, conjugate ductile shear zones developed during partial melting could therefore initiate at angles <45° to the shortening direction and resemble field structures ascribed to 'melt-enhanced embrittlement' (e.g. Davidson et al., 1994), without the requirement for truly dilatant brittle fracture. However, if the adjacent matrix also deforms, as expected in high-grade rocks, the angle between the shear zones containing the shortening direction increases with increasing bulk strain. For angles >90° between the conjugate pairs, the mean stress in the weaker shear zones is again greater than in the matrix (e.g. Figs. 5 and 6). The predicted feedback effect is therefore only transient for such a scenario, but new melt-enhanced shear zones could always nucleate at a more favourable angle to repeat the cycle.

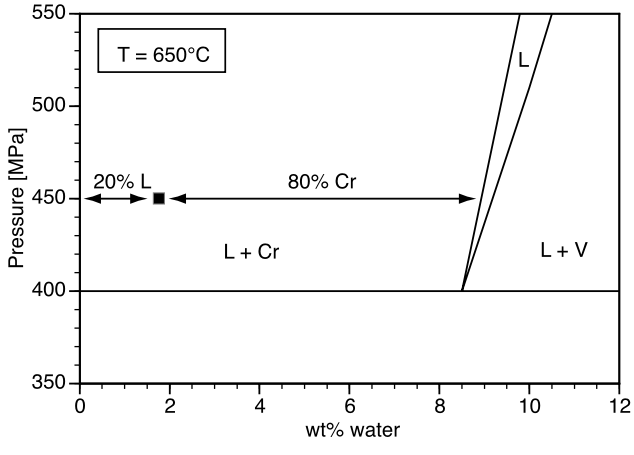

Fig. 9. Effect of increased pressure on melt percentage, derived from Fig. 8. L is liquid, Cr is crystals and V is vapour.

6. Conclusions

This study considers parameters that control shear zone development in viscoelastic materials and the mean stress distribution that should be developed. It is established that the initial viscosity contrast between the introduced weak inclusions and the matrix does not have an important effect. Power-law rheology does promote localisation compared with linear viscous rheology, but the effect is not dramatic. In the current experiments, rapid establishment of a well-defined pattern of conjugate shear zones requires strongly strain-softening behaviour, but even then the increase in strain in the shear zones relative to the matrix is only around 20%. The extreme strain localisation commonly observed in natural examples is still not adequately explained. Mechanisms for strong strain softening related to superplasticity involve a decrease in the stress exponent of power-law flow, approaching linear viscous behaviour, and, as noted above, this is not conducive to further localisation.

For viscoelastic rheology (i.e. no mean stress sensitivity), the conjugate ductile shear zones initially make an angle of 90° to each other and rotate away from the shortening direction with increased bulk strain. Especially for the most favoured case of a strain-softening material, the mean stress is higher in these extending weaker shear zones. If the bulk rock is water-saturated and close to melting, this higher effective pressure promotes melting and could therefore localise the sites of melt formation. For shear zones developed according to this mechanism, the observed preservation of leucosomes in the shear zones is unlikely to be due to accumulation, since this would require advection of melt against the prevailing pressure gradient. It is more likely to reflect preferential sites of initial melting, there being positive feedback between melting, decrease in effective viscosity and increase in local mean stress in the shear zone. Overall, melting at a specific depth is controlled by temperature and bulk composition, but local sites of melting may be determined by the heterogeneous

distribution of mean stress. Any attempted migration of the melt out of the shear zone would lead to crystallisation, so that melt should remain trapped in the shear zones and continue to localise deformation. For stretching shear zones, melt migration along shear zones may be promoted by the pressure gradient toward the shear zone tips, the positive feedback effect assisting propagation. Waning deformation and decrease in tectonic stress promotes freezing of the melt fraction, now seen in outcrop as leucosomes outlining the heterogeneous shear zone pattern.

Acknowledgements

Thanks to Djordje Grujic for stimulating discussions on the initiation of shear zones in partially molten rock during our period of analogue modelling and to Alan Thompson for discussions of melting reactions and their dependence on pressure (and many other variables). Peter Cobbold and Aaron Yoshinobu are thanked for thorough reviews that helped improve both the presentation and the structure of the paper. This paper is dedicated to Ron Vernon, whose critical enthusiasm for geology in general, and particularly for the interactions between deformation, metamorphism and melting, has had a lasting influence since my first short but intense stay at Macquarie University doing microprobe analyses for my PhD, now quite a few years ago.

References

Baumann, M.T., 1986. Verformungsverteilung an Scherzonenenden: Analogmodelle und natürliche Beispiele. Ph.D. thesis, ETH Zürich.

Baumann, M.T., Mancktelow, N.S., 1987. Initiation and propagation of ductile shear zones. Terra Cognita 7, 47.

Bowden, P.B., 1970. A criterion for inhomogeneous plastic deformation. Philosophical Magazine (Series 8) 22, 455–462.

Brown, G.C., Fyfe, W.S., 1970. The production of granitic melts during ultrametamorphism. Contributions to Mineralogy and Petrology 28, 310–318.

Brown, M., Solar, G.S., 1998. Shear-zone systems and melts: feedback relations and self-organization in orogenic belts. Journal of Structural Geology 20, 211–227.

Brown, M., Averkin, Y.A., McLellan, E.L., Sawyer, E.W., 1995. Melt segregation in migmatites. Journal of Geophysical Research 100, 15,655–15,679.

Brun, J.P., Cobbold, P.R., 1980. Strain heating and thermal softening in continental shear zones: a review. Journal of Structural Geology 2, 149–158.

Carreras, J., Cobbold, P.R., Ramsay, J.G., White, S.H., 1980. Shear zones in rocks. Journal of Structural Geology 2, 1–287.

Casey, M., 1980. Mechanics of shear zones in isotropic dilatant materials. Journal of Structural Geology 2, 143–147.

Cobbold, P.R., 1977. Description and origin of banded deformation structures. II. Rheology and the growth of banded perturbations. Canadian Journal of Earth Sciences 14, 2510–2523.

Davidson, C., Schmid, S.M., Hollister, L.S., 1994. Role of melt during deformation in the deep crust. Terra Nova 6, 133–142.

Fleitout, L., Froidevaux, C., 1980. Thermal and mechanical evolution of shear zones. Journal of Structural Geology 2, 159–164.

Grujic, D., Mancktelow, N.S., 1998. Melt-bearing shear zones: analogue experiments and comparison with examples from southern Madagascar. Journal of Structural Geology 20, 673–680.

Hobbs, B.E., Mühlhaus, H.-B., Ord, A., 1990. Instability, softening and localization of deformation. In: Knipe, R.J., Rutter, E.H. (Eds.). Deformation Mechanisms, Rheology and Tectonics. Geological Society Special Publication 54, pp. 143–165.

Holtz, F., Johannes, W., 1994. Maximum and minimum water contents of granitic melts: implications for chemical and physical properties of ascending magmas. Lithos 32, 149–159.

Hughes, T.J.R., 1987. The Finite Element Method: Linear Static and Dynamic Finite Element Analysis. Prentice-Hall, Englewood Cliffs, NJ.

Ildefonse, B., Mancktelow, N.S., 1993. Deformation around rigid particles: the influence of slip at the particle/matrix interface. Tectonophysics 221, 345–359.

Kisters, A.F.M., Gibson, R.L., Charlesworth, E.G., Anhaeusser, C.R., 1998. The role of strain localization in the segregation and ascent of anatectic melts, Namaqualand, South Africa. Journal of Structural Geology 20, 229–242.

Mancktelow, N.S., 1993. Tectonic overpressure in competent mafic layers and the development of isolated eclogites. Journal of Metamorphic Geology 11, 801–812.

Mancktelow, N.S., 1995. Deviatoric stress and the interplay between deformation and metamorphism. Abstracts of proceedings, Clare Valley Conference, Specialist Group in Tectonics and Structural Geology. Geological Society of Australia Abstracts 40, 95–96.

Mancktelow, N.S., 1999. Finite-element modelling of single-layer folding in elasto-viscous materials: the effect of initial perturbation geometry. Journal of Structural Geology 21, 161–177.

Mancktelow, N.S., Pavlis, T.L., 1994. Fold-fault relationships in low-angle detachment systems. Tectonics 13, 668–685.

Means, W.D., 1989. Stretching faults. Geology 17, 893–896.

Means, W.D., Hobbs, B.E., Lister, G.S., Williams, P.F., 1980. Vorticity and non-coaxiality in progressive deformations. Journal of Structural Geology 2, 371–378.

Poirier, J.P., 1980. Shear localization and shear instability in materials in the ductile field. Journal of Structural Geology 2, 135–142.

Poliakov, A.N.B., Cundall, P.A., Podladchikov, Y.Y., Lyakhovsky, V.A., 1993. An explicit inertial method for the simulation of viscoelastic flow: an evaluation of elastic effects on diapiric flow in two- and three-layers models. In: Stone, D.B., Runcorn, S.K. (Eds.). Flow and Creep in the Solar System: Observations, Modeling and Theory. Kluwer Academic Publishers, Dordrecht, The Netherlands, pp. 175–195.

Ramsay, J.G., Graham, R.H., 1970. Strain variation in shear belts. Canadian Journal of Earth Sciences 7, 786–813.

Schubert, G., Yuen, D.A., 1978. Shear heating instability of the Earth's upper mantle. Tectonophysics 50, 197–205.

Truesdell, C., 1953. Two measures of vorticity. Journal of Rational Mechanics and Analysis 2, 173–217.

Tuttle, O.F., Bowen, N.L., 1958. Origin of granite in the light of experimental studies in the system $NaAlSi_3O_8$–$KAlSi_3O_8$–SiO_2–H_2O. Geological Society of America Memoir 74, 153pp.